Development of a 638.6nm External Cavity Diode Laser for Scalable Ion-Trap Quantum Computing

by

Eunsu Ryu

Submitted to the Department of Electrical and Computer Engineering in partial fulfillment of the requirements for the Graduation with Departmental Distinction

at

Duke University

April 2011

Abstract

Atomic ion traps offer a promising architecture for scalable quantum information processing. External cavity diode lasers yield stable output frequency and narrow spectral bandwidth by exploiting the sensitivity of diode lasers to external optical feedback. This project aims to design and develop a high-coherence external cavity diode laser used to depopulate Yb171+ from the undesirable 2F7/2 orbital. The system uses frequency-selective optical feedback from a diffraction grating in a Littrow configuration to provide collimated, narrow-band, and frequency tunable light at 638.6nm. A piezo-electric actuator is applied to the grating to fine-tune the output frequency, while flexures are utilized for the alignment of the beam. A low-noise current source and a PID temperature controller for thermal stability are developed as a part of the system. The complete system can be easily tuned to other lasing frequencies, and will offer great benefits in laser cooling and spectroscopy of neutral atoms.

List of Exhibits

Figure 4-6: IP curve for the 650nm Digikey laser diode with optimized optical feedback

Chapter 1

Introduction

Quantum computing makes use of the probabilistic nature of the quantum world to track exponentially many instances at the same time [1]. The computational parallelism that quantum computers offer has a variety of useful applications including factorization of a large integer, search within an unsorted database, and construction of a system with fundamental security [1].

In order to make quantum computing a practical reality, it is essential to build a physical system that allows us to control quantum systems effectively to a large scale. Atomic ion traps are a promising architecture for such purpose. All basic requirements for quantum computing, which are quantum state preparation, manipulation, and read-out, have all been achieved in ion trap systems [2].

In ion trap quantum computing, hyperfine energy levels of a trapped ion is manipulated to form qubit eigenstates [2]. In order to control all possible state transitions within an ion, meticulously designed lasers targeted precisely at particular wavelengths are required [2]. The project described in this thesis contributes to the eventual goal of using yttertium ion trap to perform scalable quantum information processing. This paper seeks to answer the question: *what are the frequency and stability requirements for the construction of a laser for the manipulation of hyperfine state transitions in an ion trap?*

In particular, this paper presents the design, construction, and stabilization of a tunable, narrow-bandwidth external cavity diode laser targeted specifically at 638.6nm corresponding to the $^1D[5/2]_{5/2} \leftrightarrow {}^2F_{7/2}$ state transition. This transition is used to remove the ion from the $^2F_{7/2}$ orbital resulting from collision with ambient particles. The 638.6nm laser would allow a fast recovery of a trapped ion from an undesirable state transition, and hence enhance efficiency of the overall system.

Chapter 2 presents a brief background in laser theory. Chapter 3 presents design considerations for the construction of the laser head. Chapter 4 presents the physical implementation of the design, and Chapter 5 presents potential future work and conclusion

.

Chapter 2

Background

2.1 The Ytterbium Ion Energy States

A diagram for the hyperfine energy (valence) level structure for the $^{171}Yb^{+}$ is given in Figure 2-1.

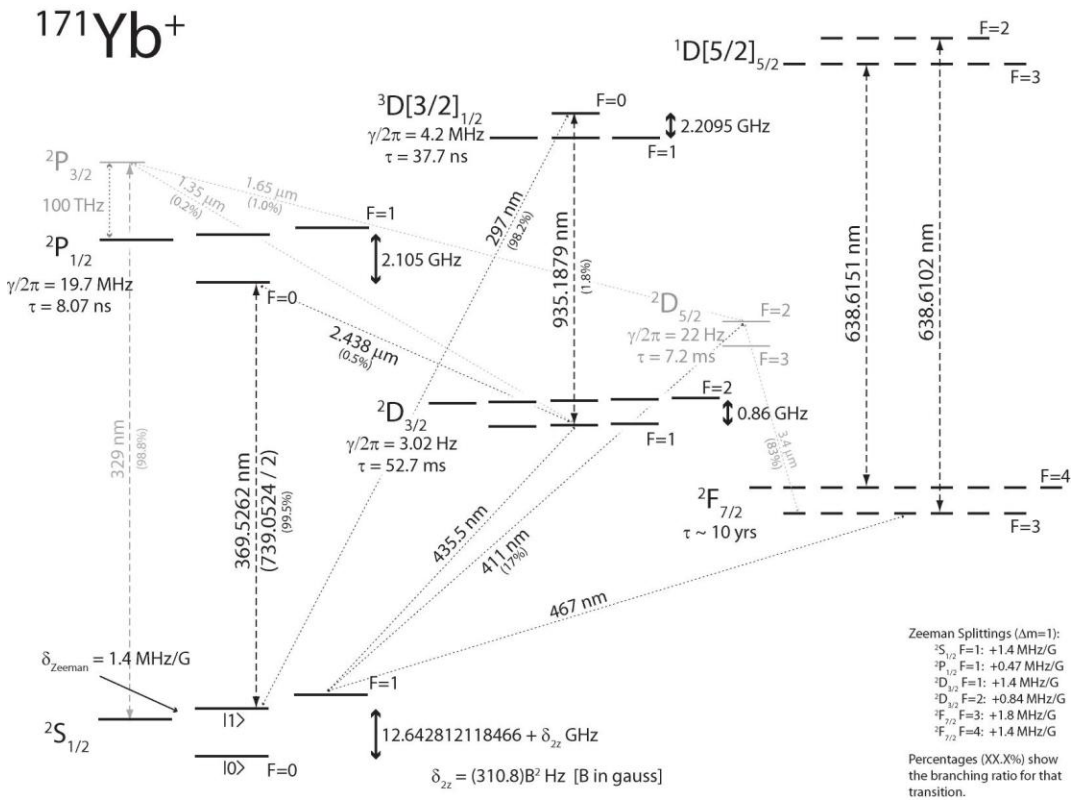

Figure 2-1: Hyperfine energy levels of the $^{171}Yb^{+}$ ion [3]

Due to the scattering of a trapped ytterbium ion with ambient particles such as hydrogen, the ion often moves to the $^{2}F_{7/2}$. This state is known to have a significantly longer lifetime (indicated "10 years" in the figure) compared to the other possible state transitions. Without the presence of a laser that induces transition to the $^{1}D[5/2]_{5/2}$ orbital, multiple ions will accumulate in the $^{2}F_{7/2}$ state over time. Hence,

in order to ensure the efficiency of quantum computation which makes use of the principal transitions between the $^2S_{1/2}$ and the $^2P_{1/2}$ states, it is necessary to remove the ion from the $^2F_{7/2}$ state as soon as such transition occurs. This thesis focuses on the design of a 638.6nm laser for the fast recovery an ion from this undesirable state. and hence enhance efficiency of the overall system.

2.2 Laser Theory

This section outlines basic laser theory used extensively throughout the project.

2.2.1 Stimulated Emission

Lasers operate on the basis of stimulated emission, which occurs when an electromagnetic wave of frequency ν is incident upon an atom in an excited state [4]. A simple illustration of a two-level quantum system is presented in Figure 2-2.

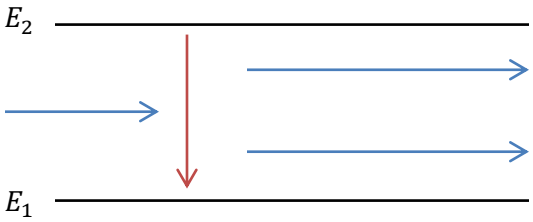

Figure 2-2: Simple two-level quantum system

The atom switches from the higher energy state to the lower energy state by emitting an electromagnetic wave that is precisely *in* phase with the incident wave, amplifying the input. In order to achieve stimulated emission, the frequency of the incident wave must be:

$$\nu = \frac{E_2 - E_1}{h}, \tag{2.1}$$

where h is the plank constant with the value $6.63 \times 10^{-34} J \cdot s$.

2.2.2 Absorption

When the radiation of frequency ν is absorbed by an atom in the lower state, the state transition from E_1 to E_2 occurs. the 638.6nm laser developed throughout the project is dedicated for the transition from the $^2F_{7/2}$ state to the $^1D[5/2]_{5/2}$ state.

2.2.3 Construction of a Laser

Population inversion is an essential step for the operation of a laser. This phenomenon refers to the injection of extra energy into the system to induce a massive number of transitions from the lower to the higher energy state, so that the number of atoms in the excited (higher) state exceeds the number of those in the ground (lower) state [5].

Since the probabilities for absorption and stimulated emission are equal, population inversion cannot be achieved in a two-level system in Figure 2-2 [5]. An example of a four-level system that induces lasing is presented in Figure 2-3.

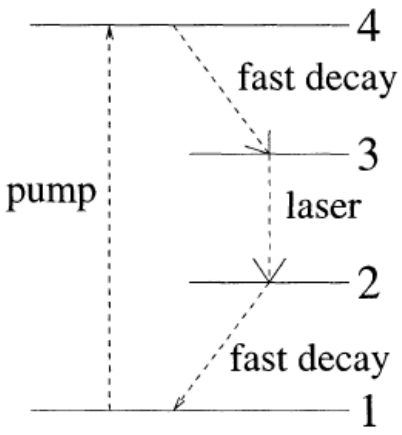

Figure 2-3: A four-level system used for population inversion [6]

In Figure 2-3, the atoms are pumped from level 1 to level 4, where they undergo a fast decay to level 3. The laser action occurs between the levels 3 and 2, and another fast decay from level 2 to level 1 occurs once stimulated emission is complete.

Figure 2-4 contains a diagram of the basic materials needed to make a laser.

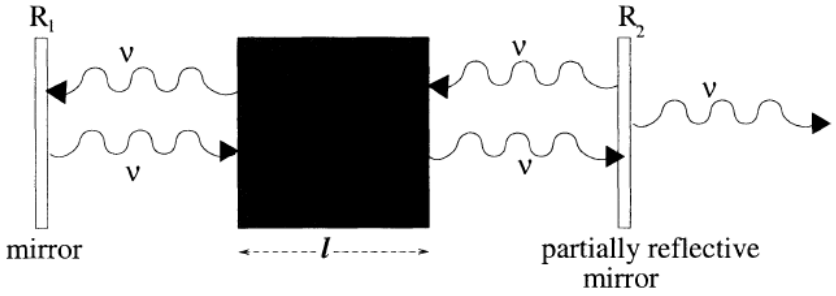

Figure 2-4: Experimental set-up of a generic laser [6]

The active material is placed in a resonant cavity between two partially reflective mirrors with reflectivity R_1 and R_2. The threshold population inversion that must be reached for spontaneous emission to occur is:

$$N_2 - N_1 = -\frac{\ln R_1 R_2}{2\sigma l}, \tag{2.2}$$

where σ is the stimulated emission cross sectional area [7]. Each time light passes through the medium across the cavity, the medium is stimulated at the frequency ν, amplifying the output.

2.3 Semiconductor Laser Diodes

Semiconductor diode lasers offer advantages in that they are cheap, small, and compact. However, semiconductor diode lasers alone are not suitable for manipulating qubits in an ion-trap quantum computer due to the lack of coherence. Figure 2-5 illustrates a simple schematic for a semiconductor pn-junction laser diode.

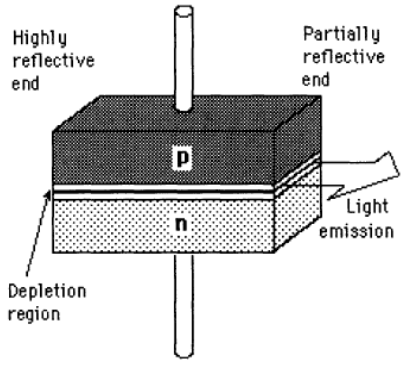

Figure 2-5: Semiconductor pn-junction laser diode schematics [8]

As the energy levels for a semiconductor form valence and conduction bands with a wide variety of possible state transitions, there exists more than one possible output wavelength [5].

Chapter 3

Laser Head Design Considerations

The goal of this section is to outline the underlying design principles for a tunable, narrow-bandwidth laser used to manipulates qubits in ion-trap quantum computers. Arguments upon which the this laser is constructed is presented along with detailed analyses. The analyses presented throughout this section can be used to create lasers tuned to wavelengths other than 638.6nm. The actual implementation of the design at 638.6nm is presented in Section 4.

3.1 Design Goals

The goal of this project is to design a low-cost laser to manipulate hyperfine energy eigenstates for ion-trap quantum computing. Specifically, the spectrum of the laser output must be narrow enough to induce state transition of an ytterbium ion, and must be stabilized, meaning that the frequency output must be time-invariant.

As hyperfine quantum states of a trapped ion necessitate high-coherence, specific frequency inputs to induce state transitions, the output of the laser must have a narrow bandwidth. According to Taehyun Kim, an ion-trap expert at Multifunctional Integrated Systems Technology, lasers used for state transitions require minimum precision on the order of a fraction of a nanometer in wavelength [9].

It should also be noted that the operation of pn-junction is highly dependent on temperature. As external current is injected to a laser diode to induce population inversion [5], energy resonating inside the laser cavity (the two-mirror system in Figure 2-4) generates heat inside the lasing medium, and hence increases temperature over time. Such variation in temperature shifts the lasing mode of the diode laser [5], and hence results in unstable laser operation. Specifically, increase in temperature will make the output frequency unstable, making the laser unusable for ion-trap quantum information processing. Stabilizing the laser to the optimal temperature is therefore essential.

3.2 Design Choice

As explained in Section 2.3, commercially available laser diodes have broadband spectrums, which make it impractical for the use in state transitions. In order to compensate for this drawback, it is necessary to stimulate the lasing medium with photons of a specific frequency. This can be achieved by providing an optical feedback to the lasing medium. The feedback will contain a certain range of frequency much narrower than the bandwidth provided by the laser diode alone. Throughout this section, we propose an external cavity diode laser, which gives additional degree of control over the spectrum of a laser diode by adding a diffraction grating as a frequency selective filter.

3.2.1 Diffraction Grating as a Frequency Selective Filter

A (reflective) diffraction grating is a frequency-selective filter that reflects lights with different wavelengths at different angles. Figure 3-1 illustrates a beam incident on diffraction grating along with its mth order diffraction associated with the wavelength λ.

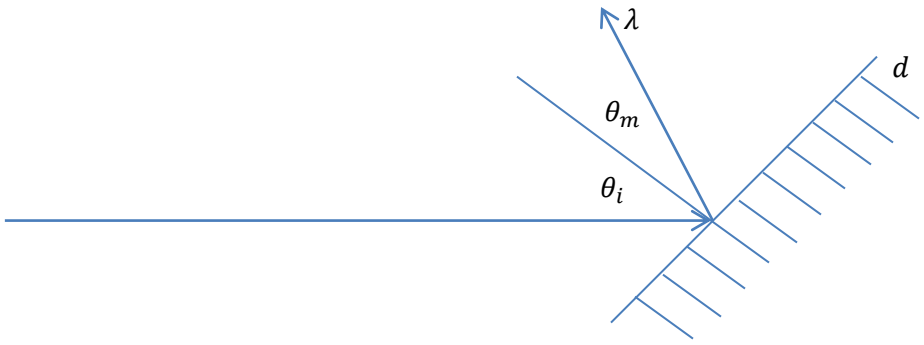

Figure 3-1: Diffraction grating

The relationship between the incident angle, wavelength, and diffracted angle for a diffraction grating is given by the equation [5]:

$$(\sin\theta_i \pm \sin\theta_m) = dm\lambda, \tag{3.1}$$

where θ_i is the incident angle with respect to the normal of the grating, θ_m is the angle of the mth order diffracted beam, λ is the wavelength corresponding to the order m, and d is the spatial frequency of the grating in rulings/nm.

Specifically, we focus on the *first* order diffraction along the optical axis, that is, collinear with the incident beam. In this configuration (called *Littrow* configuration), (2.3) becomes [5]:

$$2 \sin \theta_L = d\lambda. \tag{3.2}$$

Hence, to achieve a given wavelength λ in the Littrow configuration, one must tune the incident angle to θ_L. As a result, the first order diffraction along the incident beam will have the wavelength λ.

3.2.2 External Cavity Diode Lasers

External cavity diode laser uses a diffraction grating to provide an additional cavity outside of the lasing medium, so as to allow the user to control the spectrum of the laser output. Figure 3-2 shows a schematic for an external cavity diode laser.

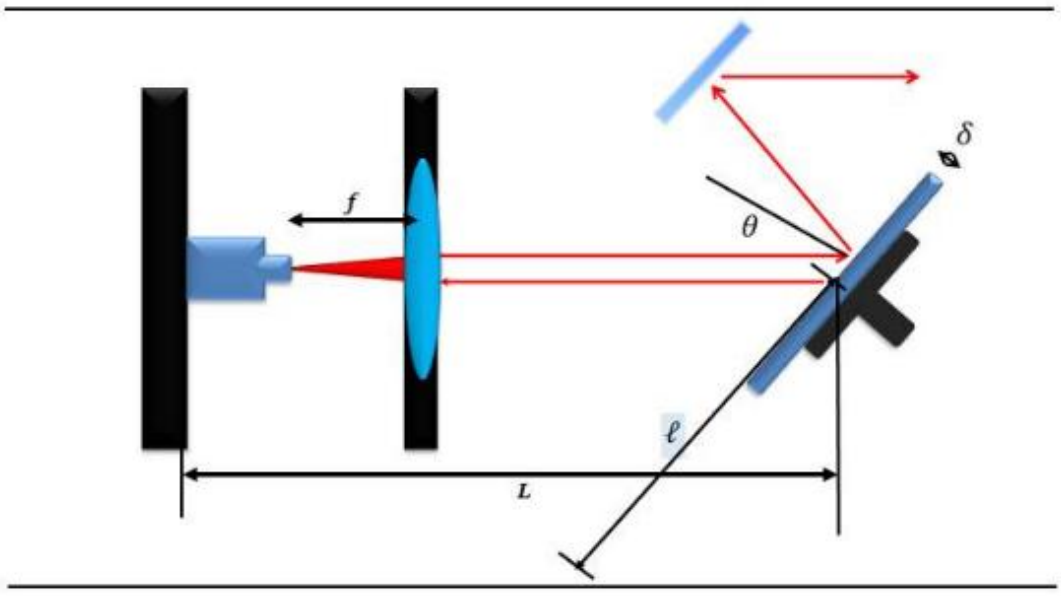

Figure 3-2: External cavity diode laser schematics

The introduction of a reflective diffraction grating adds an extra (external) cavity of length L to the system. This external cavity introduces another set of resonating modes similar to that shown in Figure 2-4. But since there can only exist an integer multiple of half a wavelength inside the cavity, the maximum distance between the two resonating modes (free spectral range) is:

$$FSR = \frac{c}{2L}. \tag{3.3}$$

3.3 Analysis of the Gain Profiles

This section is dedicated for the analysis of the above four gain profiles using the parameters given in Figure 3-2. We will derive the four important gain profiles for external cavity diode lasers.

3.3.1 Analysis of the Grating Profile

Assume that the collimating lens is positioned distance f (focal length) apart from the aperture of the laser diode. We first note that the output of the laser diode can be modeled as a Gaussian beam with intensity [5]:

$$I(\rho, z) \sim \exp\left(\frac{2\rho^2}{W^2(z)}\right),$$

where z is the distance along the optical axis, ρ is the distance along the plane normal to the optical axis, and the beam width $W(z)$ is given by [5]:

$$W(z) = W_0\sqrt{1 + \left(\frac{z}{z_0}\right)^2},$$

where W_0 is the window size specific to the laser diode, and the Rayleigh length z_0 is [5]:

$$z_0 = \frac{\pi W_0^2}{\lambda}.$$

Using paraxial approximation, we assume that the returning beam (optical feedback) is parallel to the original diode output. Since the distance between the diode and the lens is the focal length f, we say that the arriving beam is distance $f\alpha$ away from the original beam, where α is the sum of the incident and the diffraction angle.

Figure 3-4 illustrates the described situation:

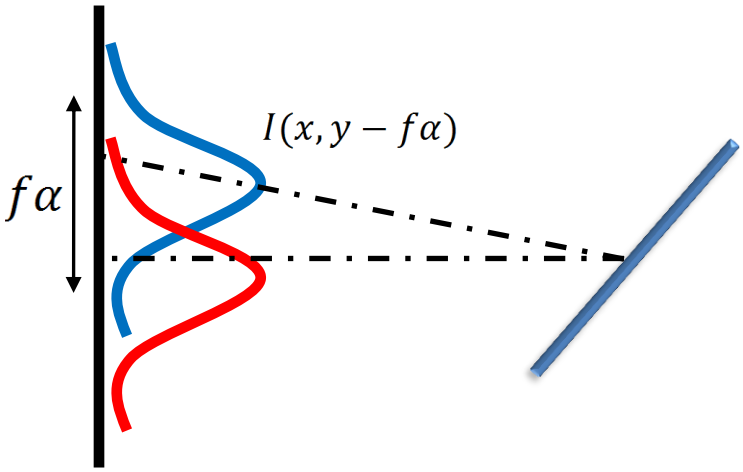

Figure 3-3: Optical feedback as a paraxial approximation

The overall feedback profile provided by the grating is then:

$$G \sim \int I(x,y) I(x, y - f\alpha) dx dy,$$

which has a Gaussian shape with width:

$$\sigma = \frac{W_0 \nu_0^2 d \cos\theta}{\sqrt{2} c f}, \tag{3.4}$$

where ν_0 is the center frequency, d is the grating frequency, and θ is the Littrow angle.

3.3.2 Analysis of the Internal and External Cavity Modes

Internal and external cavity modes are functions of the cavity length and the reflectivity of the mirrors on both edges of the respective resonator. The intensity pattern has the form [5]:

$$I_{cav} = \frac{I_0/(1 - |r|^2)}{1 + \left(\frac{2F}{\pi}\right)^2 \sin^2 \frac{\pi \nu}{\nu_F}}, \tag{3.5}$$

where ν_F is the free spectral range, and the finesse F is given by [5]:

$$F = \frac{\pi \sqrt{|r|}}{1 - |r|},$$

for the average reflectivity r.

We first note that higher value of reflectivity r increases the value of the numerator in (3.5) as well as the finesse F. Thus, higher reflectivity yields a higher amplitude, which corresponds to a greater number of photons encapsulated inside the cavity.

Figure 3-5 shows the resonating modes for two different values of the reflectivity r. Higher reflectivity results in a peak with higher intensity.

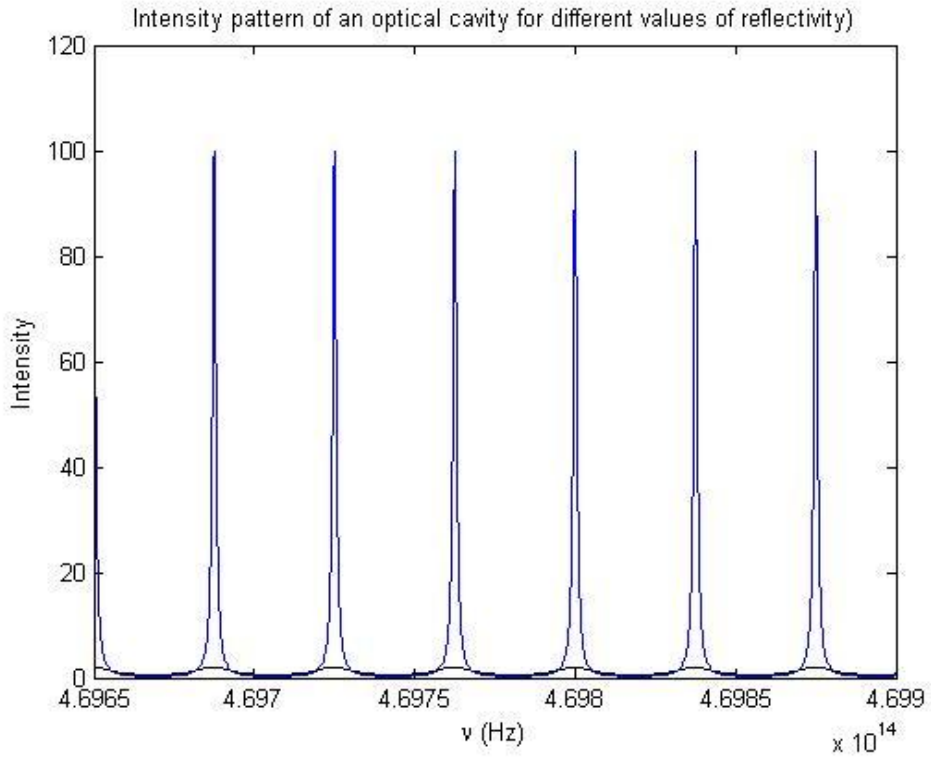

Figure 3-4: Intensity pattern for a cavity with different values of reflectivity.

Also, observe that the $\sin^2$ term in (3.5) oscillates with the frequency $\pi/\nu_F = 2\pi L/c$. A larger value of the cavity length L thus leads to more tightly packed resonating modes inside the cavity.

Figure 3-6 shows the effect of changing cavity length on the cavity mode pattern. Since the spacing between the cavity modes is the free spectral range $\frac{c}{2L}$, longer cavity length results in a narrower peak at the mode frequency.

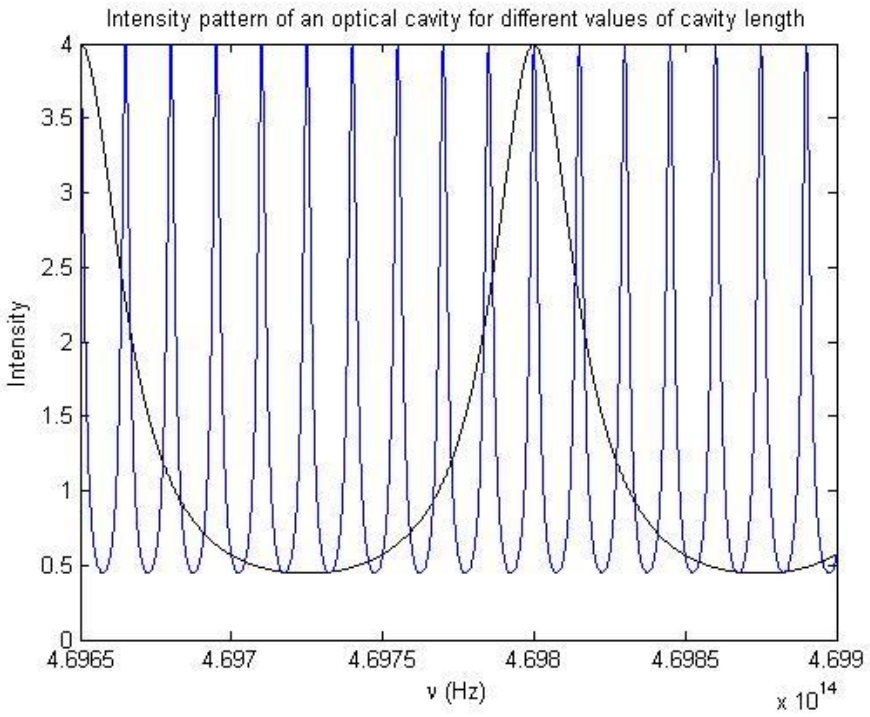

Figure 3-5: Intensity pattern for a cavity with different values of cavity lengths.

Hence we have derived the important gain parameters that characterize any external cavity diode laser. A simple schematics for the gain curves is provided in Figure 3-6.

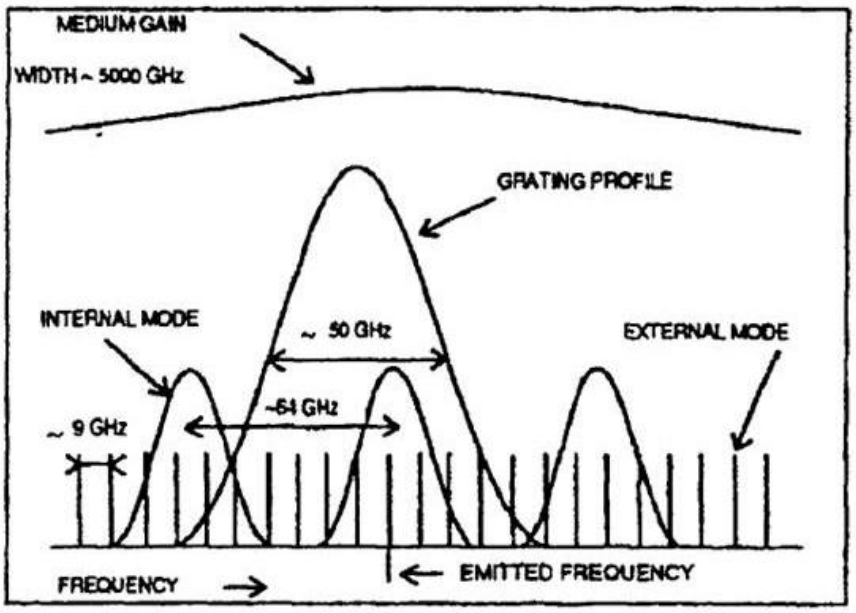

Figure 3-6: External cavity diode laser gain curves [10]

The medium gain is determined by the design of the laser diode [10]. For each value of temperature, a diode laser will have an optimal wavelength operation. Change in temperature of the lasing medium would shift the medium gain curve.

The internal cavity mode is determined by the cavity length and the reflectivity at both ends of the lasing medium [10]. Higher reflectivity results in sharper peaks, while lower reflectivity implies wider blobs [5]. As the cavity length of the lasing medium (internal cavity) is typically on the order of a millimeter, which is much smaller than typical external cavity length (order of cm), the internal cavity free spectral range (spacing) tends to be wider than those of the external cavity.

The external cavity mode is determined by the length of the external cavity defined by the diffraction grating and the back end of the lasing medium. It is also dependent on the reflectivity of the grating as well as the reflectivity at the back of the lasing medium. As the cavity length is larger than that of internal cavity, the resonating modes tend to be more tightly packed [10]

The grating profile is the range of frequencies for the optical feedback provided into the lasing medium by the diffraction grating. As will be manifested in the calculations that follow, the width of the grating profile tends to be on the order of 50 GHz for visible wavelengths [10].

It is important to note that, in linear optics, the laser output cannot exist outside the intersection of the above four curves. Also, modes farther away from the center of the grating profile will decrease in amplitude. Therefore, the bandwidth of the laser output is upper bounded by the free spectral range of the external cavity: $c/2L$.

3.4 Mechanical Considerations

In Section 3.3, we have derived the four gain curves that characterize an external cavity diode laser, and studied parameters that determine the properties of these curves. This section presents mechanical considerations used for the actual design of the laser. The goal of the mechanical design is to control the four curves as effectively as possible. In particular, we focus our attention on the control of the gain profiles provided by the diffraction grating and the external cavity.

Some design decisions are provided throughout this section.

3.4.1 Degrees of Freedom

We first take into account all the mechanical degrees of freedom in the design of an external cavity diode laser to ensure that it is possible to achieve the desired output wavelength and stability.

3.4.1.1 Collimation

In order to collimate the output of the laser diode, we place a collimating lens distance f (focal length) apart from the diode window. The design goal is to enable the movement of the lens along the plane normal to the optical axis of the laser diode, so that the user can tune the lens to align their axes. It is also desirable to allow a reasonable degree of freedom for both the lens and the laser diode along the optical axis to ensure that collimation is complete.

Also, in order to ensure that all the light from the diode is captured by the collimating lens, the numerical aperature [5] of the lens must be greater than the beam width at the focal length:

$$NA_{lens} > n \sin \theta_{div}, \tag{3.6}$$

where θ_{div} is the divergence angle determined by the design of the laser diode. Since diode lasers typically have elliptical beam shapes [10], θ_{div} must be chosen for the larger of the two divergence angles.

3.4.1.2 Alignment for Feedback

In order to ensure that the optical feedback provided by the grating stimulates the lasing medium, we used a cylinder shown in Figure 3-7 to host the laser diode and the collimating lens altogether. The cylinder will rotate with respect to its axis so that the vertical displacement between the original diode laser output and the returning optical feedback can be controlled and aligned.

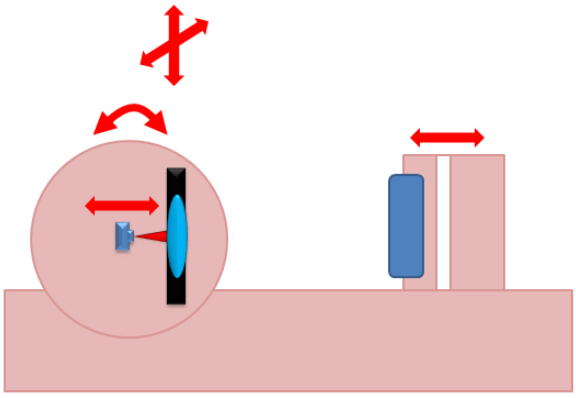

Figure 3-7: Cylinder design for optical feedback alignment

A separate lens mount will be mounted on top of the cylinder so that the lens can move along the plane normal to the optical axis. Once the alignment is complete, the cylinder will be friction-clamped to the laser head so as to prohibit further movement.

The grating is mounted on a separate platform shown in Figure 3-8 to adjust its angle.

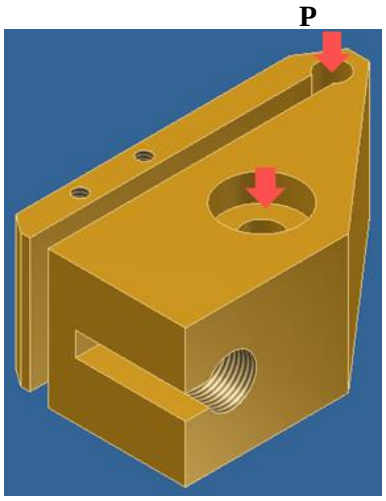

Figure 3-8: Grating mount

Note that change in the grating incident angle (Littrow angle) results in change in length of the external cavity.

3.4.2 Wavelength FineTuning

Fine-tuning of the wavelength can be achieved once optical feedback is guaranteed. This can be done by fine-tuning the Littrow angle rotating the diffraction grating with respect to the pivot point *P* shown in Figure 3-8. Since the rotation of the diffraction grating changes the length of the external cavity, the spacing between the resonator modes (free spectral range) as well as the frequencies at which the nodes are present, will shift accordingly.

In order to achieve a precision on the order of a fraction of nanometer required for state transition in ytterbium ions, we adopt a piezo-electric device. When voltage is applied, a piezo-electric device can expand and contract on the scale of nanometers [10], and hence is capable of shifting the gain curves to meet the precision requirement.

3.4.3 Length of Hinge: Tuning Two Gains at Once

Since tuning the Littrow angle of the diffraction grating changes the length of the external cavity, in order to control the gain of the whole system, we would like to have some uniform control over the gain curves presented in Figure 3-6. As the introduction of the external cavity allows two additional degrees of freedom defined by the grating profile and the external cavity resonating modes, we would like to shift these two curves in a somewhat uniform manner so as to tune the output in a predictable fashion.

The design goal is to optimize the position of the pivot point **P** in Figure 3-8 so that a small rotation with respect to **P** results in a uniform shift of the grating profile and external cavity modes: two curves move in unison. Figure 3-9 shows the set-up of the problem.

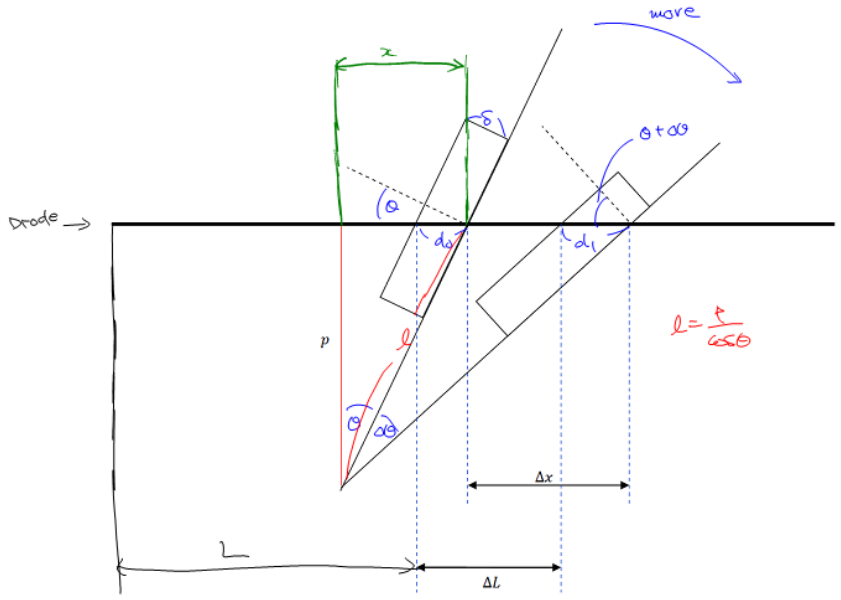

Figure 3-9: Set-up for the pivot point problem

It is assumed that fine-tuning is possible. As a result, we can safely assume that $\Delta\theta$, ΔL and Δx are all infinitesimally small. The objective is to find $\ell = p \sec\theta$.

By geometry, $\Delta \tan\theta = \tan(\theta + \Delta\theta) - \tan\theta = \Delta x/p = \sec^2\theta\, \Delta\theta$. So $\Delta x = p \sec^2\theta\, \Delta\theta$, and

$$\Delta L = \Delta x + d_0 + d_1 = (p - \delta \sin\theta) \sec^2\theta\ \Delta\theta. \tag{3.7}$$

In order for the two curves to shift in unison, it is required that wavelength shifts for the two curves induced by the rotation are equal.

For the shift induced in the external cavity modes due to change in the cavity length L, we have

$$\Delta\lambda_L = 2(L + \Delta L)/N - 2L/N = 2\Delta L/N. \tag{3.8}$$

where the integer N represents the mode number. For the shift induced in the grating gain curve due to change in the Littrow angle θ, we have

$$\Delta\lambda_G = 2d\sin(\theta + \Delta\theta) - 2d\sin\theta = 2d\cos\theta\ \Delta\theta. \tag{3.9}$$

Combining the above two expressions, we obtain:

$$p = \frac{2Ld}{\lambda_0}\cos^3\theta + \delta\sin\theta, \tag{3.9}$$

where the target wavelength $\lambda_0 = 2L/N$ is the desired wavelength, and the length ℓ can be obtained by:

$$\ell = p\sec\theta = \frac{2Ld}{\lambda_0}\cos^2\theta + \delta\tan\theta. \tag{3.10}$$

3.4.3 Temperature Considerations

Temperature of the laser system must be kept constant to prevent accidental mode hopping and to ensure that the output wavelength is stable in time. In order to achieve this functionality, we install a Paltier cooler beneath the laser head, and attach a separate control system to tune the system temperature to the optimal range. Figure 3-10 shows the system design for the overall laser system.

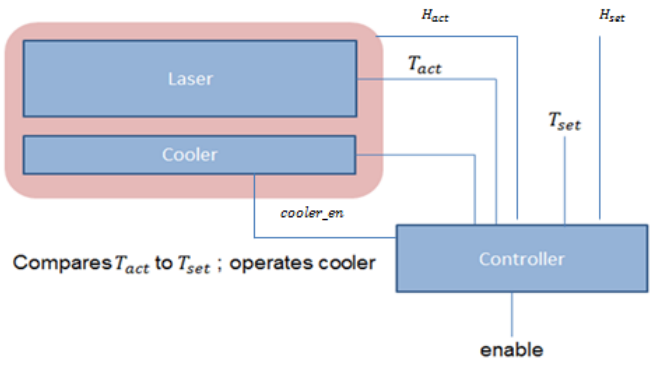

Figure 3-10: Overall laser system block diagram

The controller cools the laser system to a specified temperature, and provides an extra safety mechanism by disabling the cooler when vapor around the laser diode starts condensing.

The material must also be carefully chosen so that heat distribution is uniform over the laser head.

Chapter 4

Implementation of the Laser Head

Using the guidelines developed in Chapter 3, we now implement an external cavity diode laser tuned specifically to the wavelength of 638.6nm. This section explains the choice of components followed by numerical analysis of the parameters developed in the previous section. The data collected throughout the implementation of this laser is also presented in this section followed by discussions.

4.1 Choice of Components for 638.6nm ECDL

For the laser diode, we choose the Thorlab DL6148-030 model with optimal wavelength at 638nm, and the divergence angle of 16 degrees. This laser diode has the threshold current of $60mA$, and operating power of $40mW$. Due to the sensitivity of the DL6148-030 diode, the initial stages of the implementation were carried out using the Digikey 38-1007-ND diode with 650nm wavelength. This laser diode has threshold current 20mA and operating power 5mW. Both laser diodes operate optimally at the room temperature. Throughout the remainder of this thesis, we will assume that the medium gain gives a reasonable value at the room temperature so that the optical power is reasonably high to be able to distinguish the laser output from ambient noise.

In order to ensure that the numerical aperture of the lens is large enough to contain all the light at the focal distance, Thorlabs A230TM-A collimating lens with numerical aperture 0.55 was chosen. As the divergence angle of 16 degrees yields $n \sin \theta_{div} \approx 0.28$, condition (3.6) is satisfied. The collimating lens can capture all the light emitted from the laser diode.

As optical feedback is provided by the grating, the increased number of photons trapped inside the internal cavity makes the internal optical power far greater than that of the output. Hence, in order not to damage the diode, it must be ensured that the diffraction grating have a relatively low value of reflectivity. Following the suggestion from Peter Maunz [11], an ion-trap expert at Multifunctional Integrated

Systems Technology, we have purchased the Thorlabs GH13-24U holographic reflective grating with the density of 2500 lines/mm, and reflectivity of around 20% (s-polarization) at wavelengths around 650nm.

Table 4-1 shows the properties of different candidate materials for the body of the laser [12].

Metal	Thermal Conductivity [W/m*K]	Electrical Resistivity [uOhm*cm]	Thermal Expansion Coeff. [/C]	Density [g/cm3]	Melting Point [C]	Modulus of Elasticity [MPa]
AlBz 954	58.7 @20C	13.33 @20C	16.2e-6 @20C	7.45	1038	107000
Al	235	2.826	22.2e-6	2.7	660.4	70000
Stainless Steel 314	17.5 @100C	77 @100C	15.1e-6 @100C	7.8	~1400	193000
Brass (CZ121)	123 @100C	0.62 @100C	20.9e-6 @100C	8.47	875	97000

Table 4-1: Properties of different candidate materials

Although aluminum has the highest heat conductivity, it would be difficult to construct the spring on the grating mount (Figutre 3-8) due to its low elasticity. Stanless steel has the highest elasticity, but is not suitable for our laser due to its low heat conductivity. Brass has a high thermal expansion coefficient, which makes it unsuitable for the design. We chose aluminum bronze 954, an alloy that gives a reasonable elasticity as well as thermal conductivity.

Figure 4-2 shows the final design for the 638.6nm.

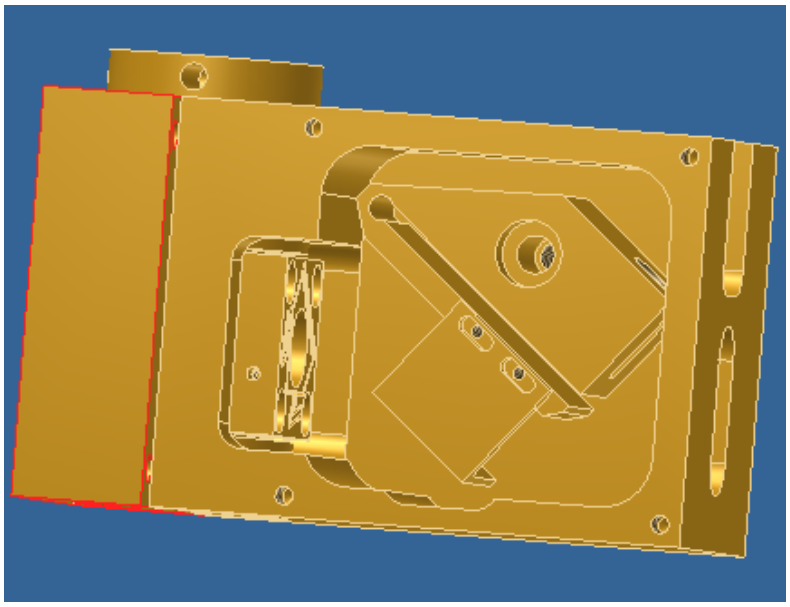

Figure 4-2: Design of the 638.6nm external cavity diode laser

The laser head is surrounded by the wall to enhance stability of operation by blocking air currents.

4.2 Analysis of Parameters

The values of the relevant parameters determined throughout Chapter 3 and by the component choices in Section 4.1 are presented in Table 4-3.

Parameter	Value
Target wavelength	638,6nm
Focal length	4.51mm
Output frequency	638nm
Beam waist	1um
Grating frequency	2400 lines/mm
Spectral bandwidth	43.8GHz
Internal cavity length	1mm
Internal cavity mode spacing	300GHz
Target frequency	469.8THz
Numerical aperture	0.55
Divergence angle	16 degrees
Rayleigh length	2m
Littrow angle	0.873 rad
External cavity length	2.08cm
External cavity mode spacing	7.23GHz
length of pivot	2.42cm

Table 4-3: List of parameters

Figure 4-4 illustrates three of the gain curves with the specified values in Table 4-3.

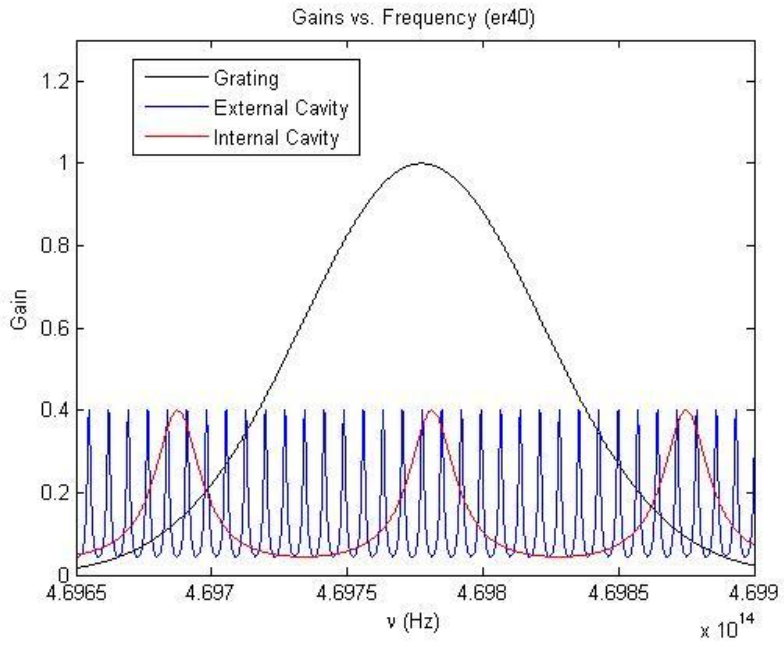

Figure 4-4: Gain curves for 638.6nm external cavity diode laser

As no value of reflectivity is provided within the datasheet for the laser diode, $r = 0.5$ is assumed throughout the analysis. In the worst case, the bandwidth of the laser output is upper bounded by the free spectral range of the external cavity resonator (7.23GHz), which corresponds to 0.009nm. In actuality, due to the highly nonlinear nature of the optical feedback and internal mechanism of the laser diode, the bandwidth will be significantly lower than this value, and will be able to satisfy the bandwidth condition for ion-trap state manipulation [9].

4.3 Optimization of Optical Feedback

In order to maximize the gain from the optical feedback from the diffraction grating, an experimental optimization method is developed and described throughout this section.

4.3.1 Feedback Optimization Method

1. Place the diffraction grating at the desired position. The angle the grating makes with the optical axis should be close to the target Littrow angle.
2. Place a photodiode along with its accompanying circuit to measure the optical power at the output. Use an oscilloscope to visually monitor the change in output power.
3. Use a function generator to generate a triangular wave at a certain frequency (e.g. 20 Hz) to modulate the current input the laser diode. This will modulate the output power of the system in the same way.
4. Turn the oscilloscope to the alternative current mode to monitor modulation only.
5. Inject current into the laser diode until it reaches threshold. Keep the current below the threshold.
6. Turn the cylinder using a solid rod until feedback is achieved. The modulation on the oscilloscope screen will display an exponential increase in output power when feedback is achieved.
7. Repeat steps 5 and 6 until no feedback is achieved.
8. Clamp the cylinder tightly and removed the rod, so that the set-up is conserved.

4.3.2 Decrease in threshold current

Figure 4-5 shows the relationship between the injection current and power output for the 650nm Digikey 38-1007-ND diode at the absence of optical feedback. The threshold current is approximately around 16mA.

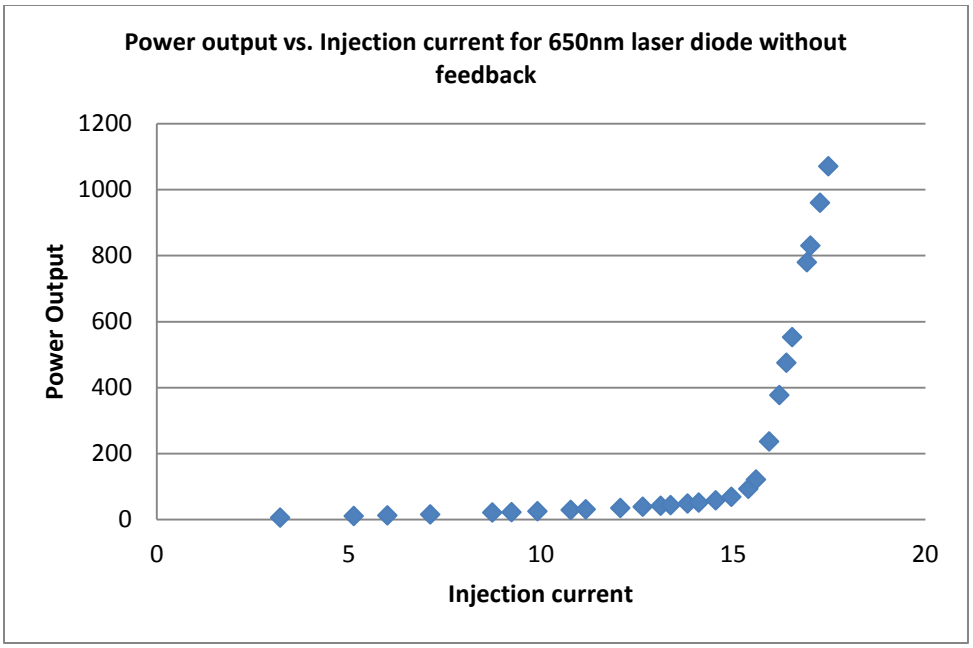

Figure 4-5: IP curve for the 650nm Digikey laser diode without optical feedback

Figure 4-6 shows the relationship between the injection current and power output for the 650nm Digikey 38-1007-ND diode with optical feedback optimized with the mechanism presented in Section 4.3.1.

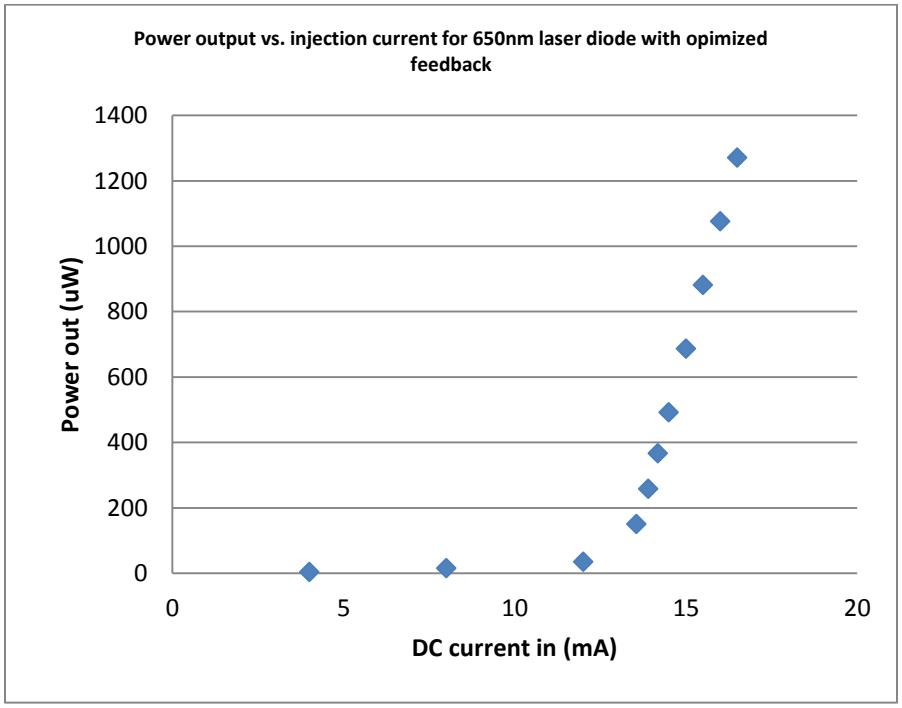

Figure 4-6: IP curve for the 650nm Digikey laser diode with optimized optical feedback

The threshold current has dropped to 13.6mA. As optical feedback is expected to decrease the threshold current by around 15% [10], the result shows that the feedback is close to optimal.

Chapter 5

Conclusion and Future Work

The project described in this thesis contributes to the eventual goal of using yttertium ion trap to perform scalable quantum information processing. This paper seeks to answer the question: *what are the frequency and stability requirements for the construction of a laser for the manipulation of hyperfine state transitions in an ion trap?*

This thesis seeks to present the design, construction, and stabilization of a tunable, narrow-bandwidth external cavity diode laser used to control atomic qubits in an ion-trap quantum computer. W e have first presented the general design of a laser to be tuned to desired wavelengths to manipulate a variety of transitions, and then implemented the design specifically at a particular value of wavelength. The implementation is specific to a laser tuned at 638.6nm, used to induce $^1D[5/2]_{5/2} \leftrightarrow {}^2F_{7/2}$ state transition. When successfully built, the laser should be capable of removing ytterbium ion from the $^2F_{7/2}$ orbital resulting from collision with ambient particles. The 638.6nm laser would allow a fast recovery of a trapped ion from an undesirable state transition, and hence enhance efficiency of the overall system.

Potential future would involve the implementation of the laser system with the actual 638nm diode. Although the author has sought to use the 638nm laser diode to construct the system, the spectrum of the output cannot be verified due to the low resolution of the optical spectrum analyzer. Prior to fine-tuning the wavelength using a piezo-electric device, the laser must be ensured to run at a single mode. More advanced optical spectrum analyzer would be required to verify the result. Temperature control and safety system was constructed to control multiple lasers simultaneously, but is not included in the thesis as the system is primarily used to control lasers other than the 638.6nm laser; 638.6nm laser does not require a complex control mechanism as it runs stably at room temperature, meaning that vapor condensation is unlikely to occur.

References

[1] Neilsen, and Chuang. Quantum Computation and Quantum Information.

[2] D. Kielpinski, C. Monroe, and D.J. Wineland. Architecture for alarge-scale ion-trap quantum computer. *Nature*, 417, 709-711, June2002.

[3] Multifunctional Integrated Systems Technology Group Wiki

[4] Shankar. *Principles of Quantum Mechanics*

[5] Saleh, and Teich. *Fundamentals of Photonics*

[6] Thon. A 674nO. Svelto. *Principles of Lasers.* Plenu, Press. 1989.

[8] C.R. Nave. Hyperphysics. Georgia State University, 2005. http://hyperphysics.phy-astr.gsu.edu/hbase/hframe.html.

[9] Taehyun Kim. Multifunctional Integrated Systems Technology.

[10] Toptica Photonics AG. DL100 Diode Laser System Manual, 2001.

[11] Peter Maunz. Multifunctional Integrated Systems Technology.